International Journal of Astronomy and Astrophysics, 2018, 8, 306-322
http://www.scirp.org/journal/ijaa
ISSN Online: 2161-4725
ISSN Print: 2161-4717

Spatial Distribution of Radiation Belt Protons Deduced from Solar Cell Degradation of the Arase Satellite

Honoka Toda[1*], Wataru Miyake[1], Yoshizumi Miyoshi[2], Hiroyuki Toyota[3], Yu Miyazawa[3], Iku Shinohara[3], Ayako Matsuoka[3]

[1]Department of Aeronautics and Astronautics, Tokai University, Kanagawa, Japan
[2]Institute for Space-Earth Environmental Research, Nagoya University, Nagoya, Japan
[3]Institute of Space and Astronautical Science, JAXA, Kanagawa, Japan
Email: *8bemm060@mail.u-tokai.ac.jp

How to cite this paper: Toda, H., Miyake, W., Miyoshi, Y., Toyota, H., Miyazawa, Y., Shinohara, I. and Matsuoka, A. (2018) Spatial Distribution of Radiation Belt Protons Deduced from Solar Cell Degradation of the Arase Satellite. *International Journal of Astronomy and Astrophysics*, **8**, 306-322.
https://doi.org/10.4236/ijaa.2018.84022

Received: October 3, 2018
Accepted: November 11, 2018
Published: November 14, 2018

Abstract

Analysis of solar-cell array panel (SAP) data from the Arase satellite orbiting in the inner magnetosphere showed a clear degradation of solar cells that could be attributed to trapped protons with energies greater than 6 MeV. Proton fluence was determined based on variations in the open-circuit voltage (Voc) of the solar cells, which we compared with that expected based on various distribution models (AP8MAX, AP9 mean and CRRESPRO quiet) of trapped protons. We found a general agreement, confirming the major contribution of trapped protons to the degradation, as well as a slight difference in the fluence expected based on the model calculations. To minimize this difference, we slightly modified the models, and found that concentrating the energetic protons on the magnetic equator provided a better agreement. Our results indicate that >6 MeV protons also has the equatorial concentration as reported for >18 MeV protons from the Van Allen Probes observation, and are interpreted as two components of the trapped protons, *i.e.*, those of solar energetic particle (SEP) origin have an anisotropic pitch-angle distribution and are confined near the magnetic equator.

Keywords

Arase Satellite, Proton Radiation Belt, Solar Cell Degradation

1. Introduction

The inner radiation belts are mainly populated by energetic protons. Recent observations with the Van Allen Probe [1] have clearly demonstrated that the

energetic protons consist of two components, *i.e*., protons of solar energetic particle (SEP) origin and those of cosmic ray albedo neutron decay (CRAND) origin [2]. Trapped protons of SEP origin have rather lower energies, and a great concentration near the magnetic equator at larger L-shells. These properties are quite important for understanding proton injection, transport, and loss processes in the inner magnetosphere. They are revealed for protons with energies greater than 18 MeV. Since proton measurement with the Van Allen Probes has a gap of proton energies between 1 and 17 MeV [3], properties of several to ten MeV protons have not been studied.

Cumulative damage from space radiation generally decreases the output power of solar cells used in space. Ishikawa *et al.* [4] reported the decrease in output current of silicon solar cells of the Akebono satellite orbiting in the inner magnetosphere, and carried out a correlation study to identify possible causes of the degradation. They found that the trapped component of energetic (>10 MeV) protons in the radiation belt is mainly responsible for the decrease in output current. Miyake *et al.* [5] [6] further analyzed the variation in output current of the Akebono solar cells between 1989 and 1996, and pointed out that the proton radiation belt was more sharply confined than that given by the AP8 model. We realized from these earlier studies that by analyzing the degradation of solar cells, we can indirectly study the proton radiation belt.

The Arase (formerly known as the Exploration of energization and Radiation in Geospace, ERG) satellite was successfully launched on December 20, 2016, from the Uchinoura Space Center. The spacecraft has apogee and perigee altitudes of ~32,000 and ~440 km, respectively, and an inclination of 32˚, allowing the spacecraft to spend the majority of its time in the radiation belts. The spacecraft has an orbital period of 570 min and is spin-stabilized with a spin period of ~8 s. The primary objective of the Arase mission is to reveal the generation mechanisms of relativistic electrons in the radiation belts [7].

The Arase satellite measures electrons within a wide energy range, whereas the measurement of ions is carried out only below 180 keV, mainly for ring current particles [8]. Its solar array panel (SAP) data clearly shows the degradation of solar cells by space radiation, probably by energetic protons in the inner radiation belt. The cover glass of the solar cells has a thickness of 0.3 mm, which means that protons with energies greater than 6 MeV can penetrate into the solar cells [9]. In this paper, we present the results of analyzing the degradation of solar cells on the Arase satellite and deduce the spatial distribution of >6 MeV protons which are never measured by particle instruments on the Van Allen Probes and the Arase satellite. We first assume that the degradation of solar cells of the Arase satellite is caused only by trapped protons. Generally, solar energetic protons and trapped energetic electrons are both responsible for the degradation of the satellite's solar cells depending on the orbit and solar activity. We discuss the possible contribution of other causes for the degradation later.

Cumulative damage from energetic particles causes the solar cell degradation, so our analysis presents only the integration along satellite orbit over a long time

and needs a given state of particle distribution. Our approach is solving an inverse problem, in which a model distribution is estimated from the integration of proton flux, and generally the solutions are not unique. We therefore start with a model distribution which is close to the solution, and then slightly modify the model for seeking a better agreement with the degradation of solar cells.

For the first step, we used three empirical models of trapped MeV protons: AP8MAX, AP9 mean (ver. 0.0), and CRRESPRO quiet. The standard space environment specifications used for spacecraft design have been provided by NASA's AE8 and AP8 models for decades. They were developed from measurements accumulated by numerous satellites in the 1960s and 1970s. There are well-known limitations on their performance, and the need for a new trapped radiation and plasma model was recognized by the engineering community some time ago. To address this challenge, a new set of models, denoted AE9/AP9/SPM, for energetic electrons, energetic protons and space plasma was recently developed [10]. The CRRES satellite provided observation of energetic particles from July 1990 to October 1991 in the inner magnetosphere [11]. An intense solar proton event and subsequent geomagnetic storm drastically changed the trapped particle environment in March 1991. The CRRESPRO quiet model was developed based on proton data obtained before the event.

We have organized the rest of the paper as follows. The data used and method to deduce variation of proton fluence from the degradation of solar cells are described in the next two sections. Our approach is not based on direct particle measurement, and we need some analysis on performance of solar cells to deduce the proton fluence. We then compare the temporal variation of proton fluence with that expected from various model distributions. Finally we discuss probable interpretation of our results on proton fluence and spatial distribution of >6 MeV protons.

2. Data

The open-circuit voltage Voc, short-circuit current Isc, and voltage and current at maximum power, Vmp and Imp, are generally used for describing the I - V characteristics of solar cells [12]. The output current is almost identical to Isc for a wide range of operating voltages as long as the solar cells are operated at a voltage lower than the Vmp. The output current begins to decrease near the Vmp. When the operating voltage exceeds the Vmp and comes close to the Voc, the output current drastically decreases towards zero. The solar cell system of the Arase satellite is operated between the Vmp and Voc, so that the voltage decreases slightly and the current increases significantly when more electric power is consumed by the satellite's systems.

When energetic particles collide with solar cells, they penetrate into the cells and damage the inside with scratches, causing a reduction in electric power. For this reason, the efficiency of solar cells decreases as the radiation exposure increases. This effect accumulates year by year, and its influence is greater in the early stage of operation. Accumulated radiation damage causes a decrease in all

four solar cell parameters: Voc, Isc, Vmp and Imp. As the damage accumulates, the output voltage of the Arase satellite decreases towards Vmp and the current increases towards Imp if the satellite needs constant electric power.

Figure 1 shows the output voltage (upper panel) and the current (lower) from the solar cells of the Arase satellite from its launch through to March 31, 2018, which is all the data used in this study. The satellite has four SAPs and the total output current from the four panels is presented. The SAPs are covered by InGaP/InGaAs/Ge ZTJ solar cells from SolAero Technologies Corporation. Corrections for incident solar light are already made for variations in the SAP's orientation and for seasonal variations in the radial distance from the sun. The cover glass of the solar cells has a thickness of 0.3 mm, which means that protons with energies greater than 6 MeV can penetrate into the solar cells [9].

The overall trend of the voltage and current variation shown in Figure 1 is consistent with that expected from the degradation of solar cells due to accumulated damage from space radiation. The voltage decreased and the current increased. However, particle fluence is not the only factor affecting the output of solar cells. The output voltage and current are also affected by the temperature of solar cells, which ranges widely from low to high values for an Earth-orbiting satellite. Voc decreases under high temperature conditions, although Isc is only slightly affected. To precisely deduce the radiation effect, it is necessary to carefully evaluate and remove the effect of temperature variation.

Since the SAPs are well thermally isolated from the satellite, there are two sources of temperature variation. One is due to the effects of the Earth. To avoid these effects, we sorted the data based on two orbit conditions. We selected data taken at more than 4.0 Re from the Earth's shadow. The SAPs are cooled down in the shadow and it takes a certain amount of time to reach thermal equilibrium again in sun-lit conditions. We also selected data taken at a radial distance of more than 5.0 Re from the Earth for the purpose of minimizing the effect of the Earth's albedo and heat radiation.

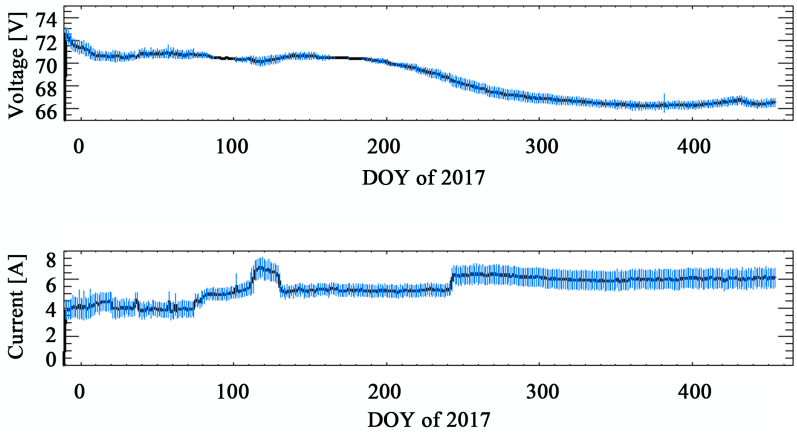

Figure 1. Variation of solar cell output voltage (upper panel) and current (lower panel) of the Arase satellite from its launch to March 2018. Blue vertical lines indicate the standard deviation.

The sun is another source affecting the SAP's temperature. Heat input from the sun varies between the aphelion (early July) and the perihelion (early January) of the Earth. We needed to model the temperature variation, since heat input from the sun is unavoidable and there are no temperature sensors on the SAPs. The method is described later.

3. Analysis

To deduce the proton fluence, we first drew a curve of the I - V characteristics passing through the daily average voltage and current of the SAPs, as presented in Figure 1. The I - V curve is expressed by an exponential function. Then we determined Voc for the day at the point of I = 0 in the I - V plane. Figure 2 shows the relative variation of the daily Voc from that at the beginning of life (BOL). Vertical bars represent the standard deviation for the daily average. We used the Voc variation in this study, since Voc is the most sensitive to particle fluence among the parameters describing I - V characteristics. The data sheet for the ZTJ cells gives a 5% decrease in Voc, but a 2% decrease in Isc from the BOL for fluence of 1014 e/cm^2.

Fast decrease and rather stable periods are alternately repeated for the Voc variation in Figure 2. Fast decrease periods may correspond to large fluence and stable periods to small fluence. Figure 3 shows an example of Arase's orbits on DOY 76 (black lines) and DOY 151 (red lines) in geomagnetic coordinates. Orbits in the southern hemisphere are folded up to the northern hemisphere. The Arase satellite entered the heart of the proton radiation belt (*i.e.*, around L = 1.5 on the Equator) on DOY 151, but did not do so on DOY 76. The same variation in orbit is repeated with a period of about 8 months due to orbit precession. Faster decrease of Voc was expected on DOY 151, but the fact is that Voc was just as stable as it was on DOY 76.

The deviation from the expected fast decrease and stable periods demonstrates that particle fluence is not the only factor controlling Voc. The temperature of the SAPs should be highest around early January and lowest around early July due to the eccentricity of the Earth's orbit around the sun. The lower temperature

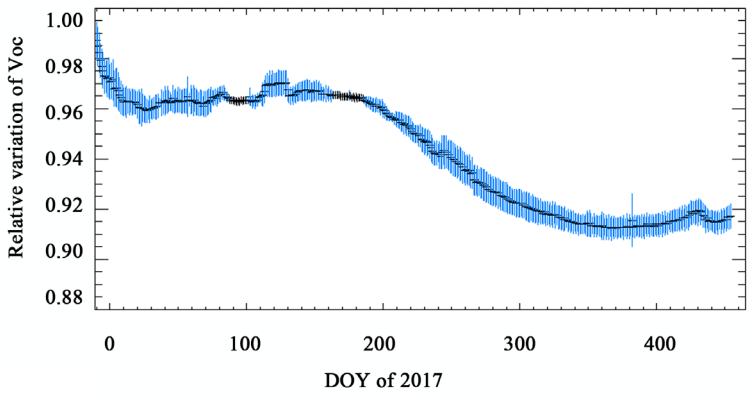

Figure 2. Daily averaged Voc from the satellite's launch to March 2018. Blue vertical bars indicate the standard deviation.

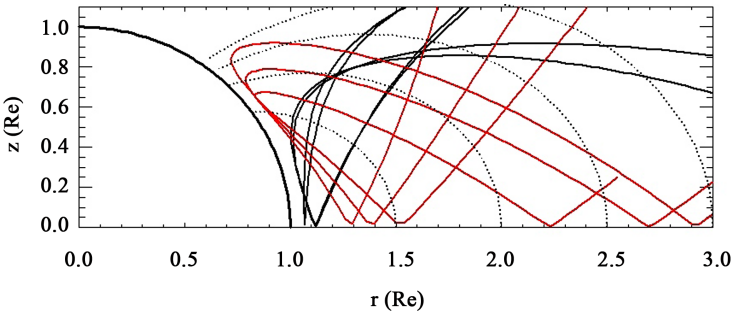

Figure 3. Orbits of the Arase satellite on DOY 76 (black line) and DOY 151 (red line) in geomagnetic coordinates. Orbits in the southern hemisphere are folded up to the northern hemisphere.

on DOY 151 compared to that on DOY 76 has the effect of increasing Voc, which may compensate for the decrease by large particle fluence around DOY 151. The data sheet for the ZTJ cell used for the Arase satellite shows a 0.23% - 0.25% decrease in Voc for a temperature increase of 1˚C during the early stage of degradation. Engineers estimated a variation of ~10˚C between the aphelion (early July) and the perihelion (early January) through thermal analysis of the satellite before its launch. Therefore, Voc variation of several percent can be attributed to temperature variation.

Since there are no temperature sensors on the SAPs, we introduced a simple model of SAP temperature based on thermal equilibrium. The SAPs are well isolated from the satellite body and heat conductance is negligible. The only heat input is from solar radiation, which varies proportionally with 1/R2, the inverse of the squared radial distance from the sun. Loss is caused only by heat radiation toward space, which is proportional to σT^4, where σ is Stefan's constant and T is the Kelvin temperature of the SAPs. If we give the amplitude of the annual temperature variation, *i.e.*, the difference between the aphelion and perihelion, then we can deduce the relative fluence from the Voc variation in **Figure 2**.

Figure 4 shows the monthly average relative fluence deduced for three cases of amplitude of the annual temperature variation. Fluence is normalized with respect to the fluence of the last month, March 2018. The relative fluence for 0˚ variation decreases from DOY 30 to DOY 130, and around the last DOY interval. Any decrease in fluence cannot be real, so some annual variation of temperature should inevitably be included in our model calculations. A case of 5˚ variation seems better, but still has a small decrease of fluence around the last DOY interval. On the other hand, the fluence increases continuously for a 10˚ variation, which is most reasonable among the three cases. Variation in the speed of increasing fluence is caused by the orbit precession, as shown in **Figure 3**, and is key to investigating the best-fitting models for the spatial distribution of energetic protons.

In this study, we first tried three empirical models for the spatial distribution of energetic protons: CRRESPRO quiet, AP8MAX, and AP9 mean (ver. 0.0). Then, we modified these models seeking better agreement with the SAP data.

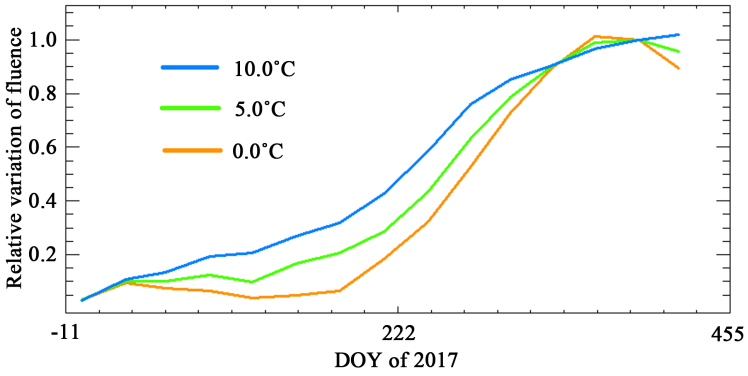

Figure 4. Relative fluence deduced from monthly averaged Voc by assuming the amplitude of annual variation of temperature as indicated in the figure. Each relative fluence is normalized by its maximum value.

The amplitude of the annual temperature variation is a free parameter in our model calculations. We changed it in 0.1˚ steps to find the amplitude that provided the best fit with the fluence variation for the given model of spatial distribution.

4. Comparison with Various Models of Proton Distribution

Figure 5 shows a comparison between the relative fluence deduced from the SAP data (blue line) and the calculated fluence from integration along the satellite orbit under the spatial distribution of energetic protons of each model (red line). The fluence is normalized by that of the last month. The fluence for CRRESPRO quiet, AP8MAX, and AP9 mean of the last month is 5.0e+11/cm^2, 1.6e+12/cm^2, and 8.1e+11/cm^2, respectively. The radiation damage coefficient (RDC) method is often used for evaluating the degradation of solar cells [13]. We are unable to use detailed figures of the solar cells in this study due to a contract with the manufacturer. Accordingly, we focus on temporal variation of the relative fluence, not the absolute values. If the RDC method were fully used, the difference among the three proton models would be quite clear. The AP8MAX has the highest fluence among the three models and would certainly give the fastest degradation.

We used the amplitude of annual temperature variation (ΔT) that provides the minimum root mean squared error (RMSE) for each model. The RMSE is largest for AP8MAX, and smallest for AP9 mean. The amplitude of annual temperature variation spreads slightly among the models, and is around 9˚. The three models differ in proton distribution (see bottom panel (C) in **Figures 6-8**), but we still obtained an overall coincidence with the fluence deduced from the SAP data, indicating that trapped protons are mainly responsible for degradation of the solar cells of the Arase satellite.

Although the RMSE differs among the three models, the deviation of the red line from the blue line is found almost at the same intervals. The first deviation is around DOY 50. The second and third deviations are around DOY 155 and

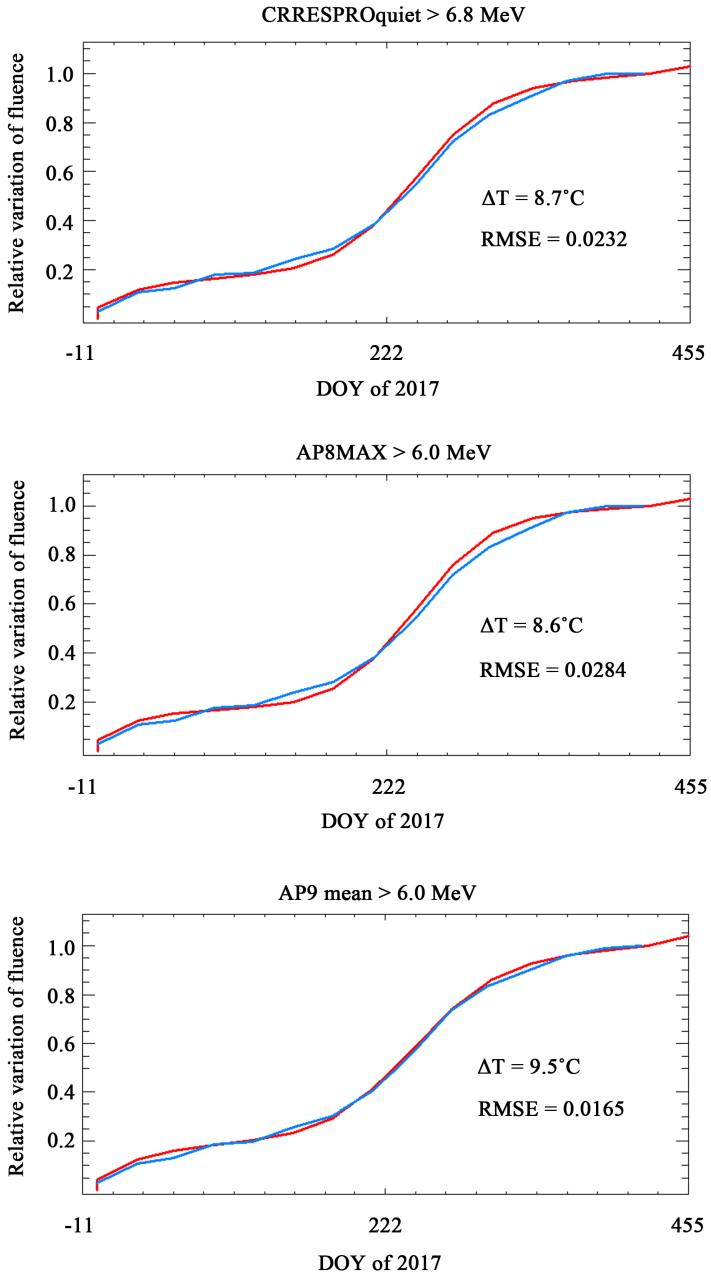

Figure 5. Comparison between the relative fluence deduced from the SAP data (blue line) and the calculated fluence from integration along the satellite orbit under the spatial distribution of energetic protons of the three models (red line). The fluence is normalized by that of the last month. We used the amplitude of annual temperature variation (ΔT) that gives the minimum RMSE (root mean squared error) for each model.

DOY 315, respectively. The relative fluence deduced from the SAP data (blue line) is larger for the deviation around DOY 155, and smaller for the other two cases. The similar pattern of deviation throughout the different models suggests a common cause. There are several possibilities, which we discuss later, but here we look at the possibility of slightly modified models for the trapped proton distribution.

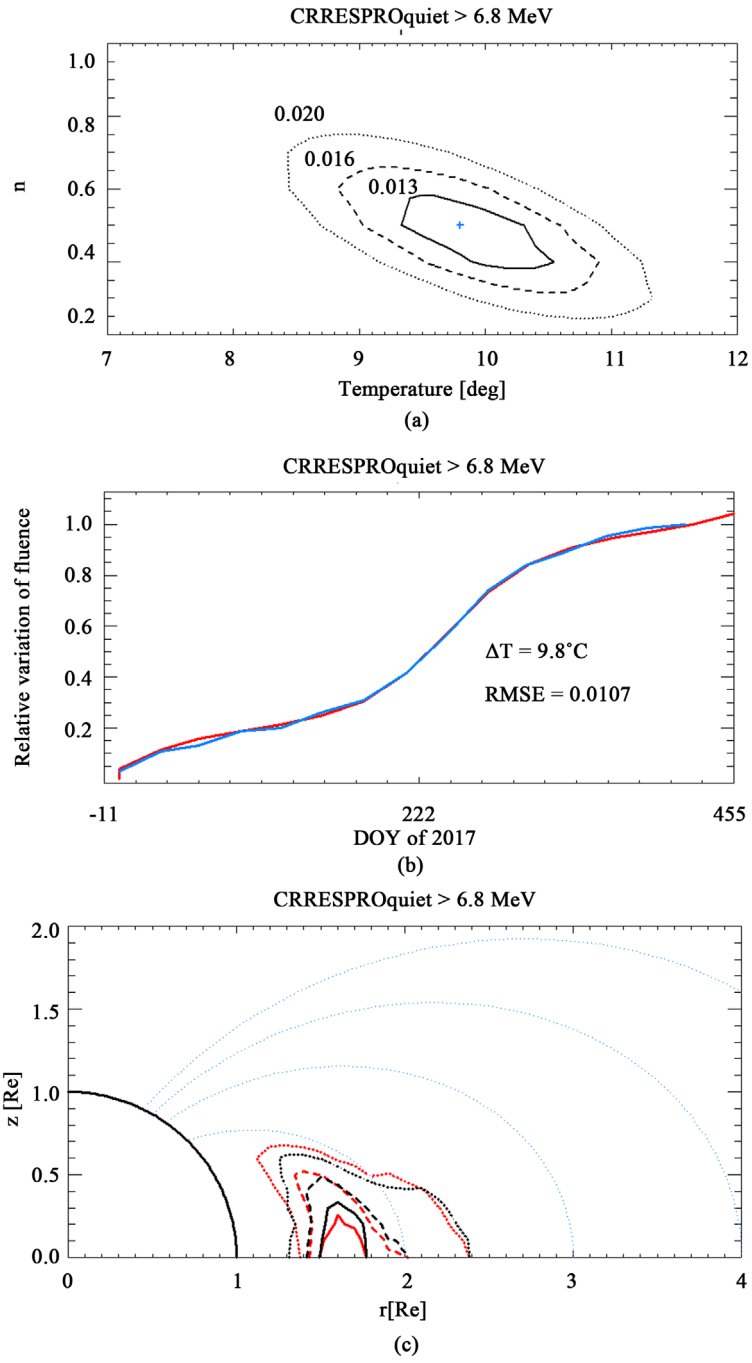

Figure 6. Summary for the modified CRRESPRO quiet model. (a) Contour map of RMSE between the relative fluence deduced from the SAP data and the calculated fluence from integration along the satellite orbit under the spatial distribution of >6.8 MeV protons of modified CRRESPRO quiet model. The RMSE is presented as a function of the amplitude of annual variation of temperature (ΔT) and n in Equation (1); (b) Variation of relative fluence deduced from the SAP data (blue line) and calculated from integration along the satellite orbit under the spatial distribution of >6.8 MeV protons of the modified CRRESPRO quiet model (red line); (c) Contour plot of the spatial distribution of >6.8 MeV protons of the original CRRESPRO quiet model (black line) and the modified model (red line). The solid, broken, and dotted lines represent 60%, 30%, and 10% of the peak flux, respectively.

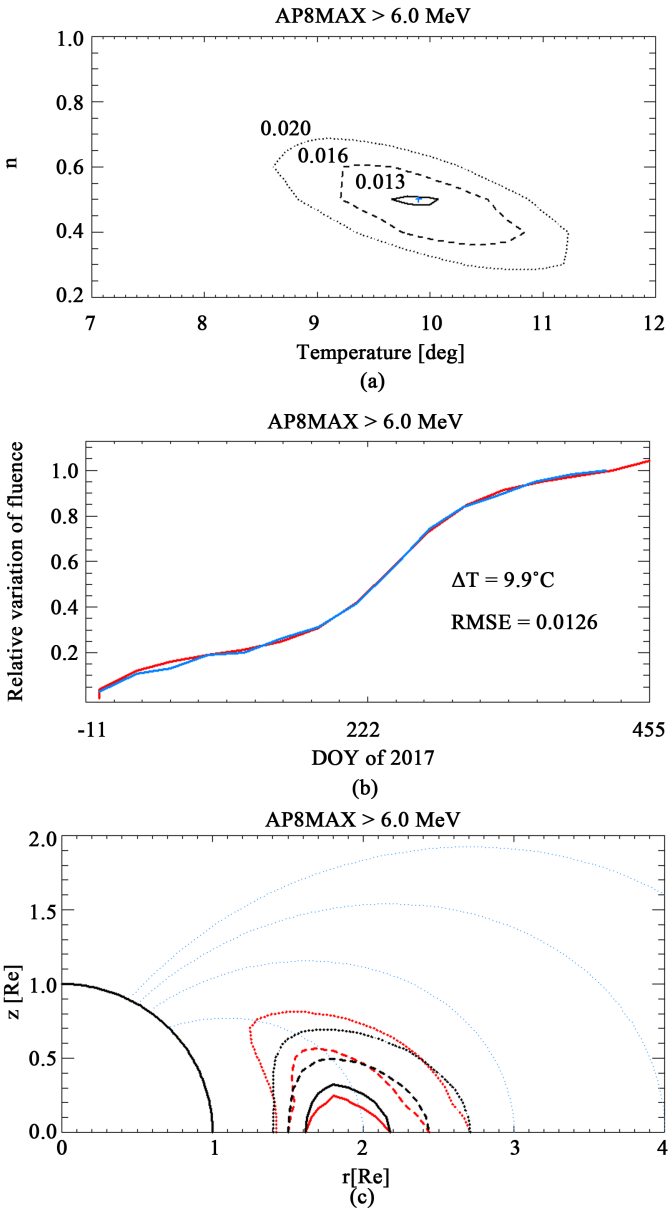

Figure 7. Summary for the modified AP8MAX model. The formats of each panel are the same as that used in **Figure 6**.

Trapped protons are generally divided into two components, *i.e.*, protons of SEP origin and those of cosmic ray albedo neutron decay (CRAND) origin. Observation by Van Allen Probes revealed that energetic protons in the inner belt have highly anisotropic pitch-angle distribution on the magnetic equator at larger L values, and that this tendency is more evident for lower-energy (26 MeV) protons. This anisotropy is interpreted in terms of a component of injected and trapped solar protons [14]. Proton energy affecting SAP degradation is more than 6 MeV, which is even lower than that in the report above, so we tried models of spatial distribution with an equatorial enhancement of proton flux at large L values. We introduced a slight modification to the three models by

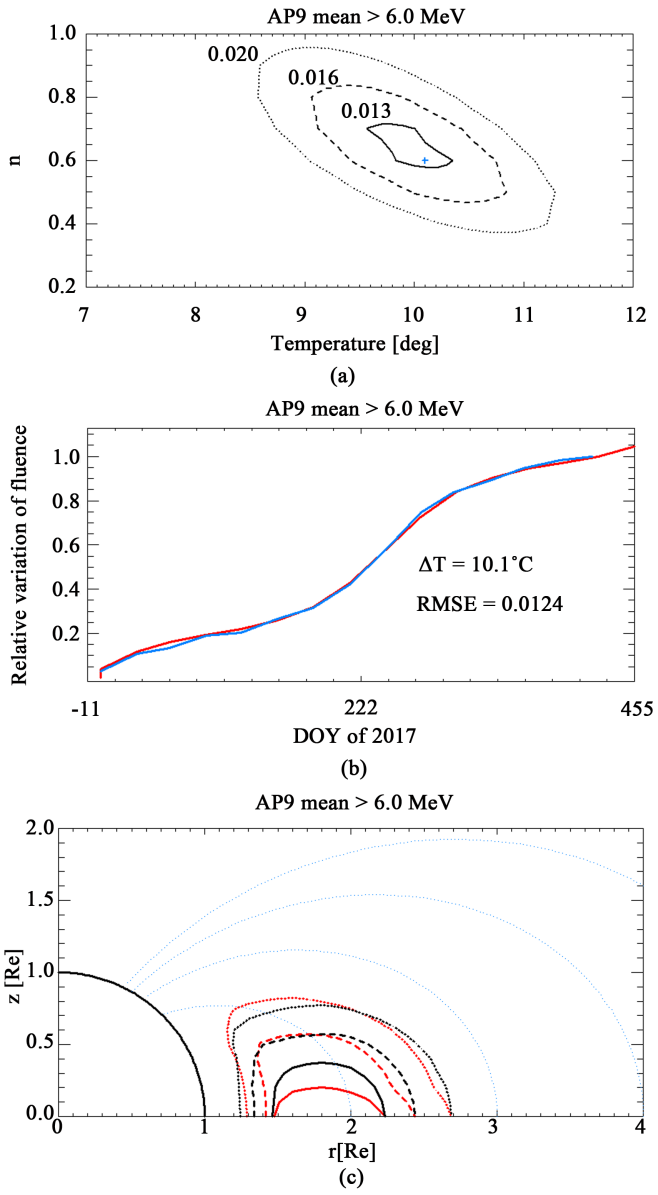

Figure 8. Summary for the modified AP9 mean model. The formats of each panel are the same as that used in **Figure 6**.

increasing the proton flux at z < 0.2 Re for L > 1.5, where z is the distance from the magnetic equator. For example, we set the proton flux at 2.0 times that of the original flux at z < 0.1 Re and 1.5 times at 0.1 Re < z < 0.2 Re of the original flux. This modification is a way of simulating one component, the SEP-derived trapped protons that are expected to concentrate near the magnetic equator.

To represent the other component, protons of CRAND origin, we also modified the proton flux distribution off the equator (z > 0.2 Re) along the field line following the equation

$$f = \left(\frac{f'}{f_{eq}} \right)^n f_{eq} \tag{1}$$

where f' is the flux of the original model at a point, and f_{eq} is the flux of the modified model on the magnetic equator with the same L value. Parameter n determines the overall distribution along the field line. The additional equatorial enhancement means that flux relative to the equator flux away from the equator decreases more drastically than the original model if we set $n > 1$. If we want only an equatorial enhancement without significantly changing the relative flux away from the equator, parameter n should be smaller than unity.

Figures 6-8 summarize the results for the modified CRRESPRO quiet, AP8MAX, and AP9 mean models, respectively. Here, we introduce a flux enhancement of 2.0 times at z < 0.1 Re and 1.5 times at 0.1 Re < z < 0.2 Re for L > 1.5 for all three models. We changed ΔT, the amplitude of annual temperature variation, by steps of 0.1˚, and n in Equation (1) by a 0.1 step, and looked for the best agreement between the fluence deduced from the SAP data and that from the spatial distribution model for energetic protons.

The top panel (A) of each figure shows a map of the RMSE as a function of the amplitude of annual variation of temperature (ΔT) and n in Equation (1). The blue mark + denotes the location of the minimum RMSE. The minimum RMSE is given in the middle panel (B). We present the monthly averaged fluence deduced from the SAP data (blue line) and the fluence integrated from the spatial distribution along the orbit in the middle panel (B) for the minimum RMSE. The bottom panel (C) of each figure shows a comparison of the spatial distribution of the original model (black lines) with that of the modified model (red lines). The original CRRESPRO quiet, AP8MAX, and AP9 mean (black lines) have a peak flux of 5.3e+5/cm^2/s, 1.1e+6/cm^2/s, and 4.7e+5/cm^2/s, respectively. The contour levels are normalized by the peak flux, and 60% (solid lines), 30% (broken lines), and 10% (dotted lines) levels are presented. Blue dotted lines show geomagnetic field lines of L = 2, 3, 4, and 5.

The minimum RMSE of 0.0107 is found at 9.8˚C and n = 0.5 for the modified CRRESPRO quiet model in Figure 6. This RMSE is better than 0.0232 for the original CRRESPRO quiet model shown in the upper panel of Figure 5. Similarly, the minimum RMSE for the modified AP8MAX and AP9 mean models is improved from the original values. We found that the deviations in the second (around DOY 155) and third intervals (around DOY 315) in Figure 5 almost vanish in the middle panel (B) of Figures 6-8. The deviation in the first interval (around DOY 50), on the other hand, does not seem to have improved in Figures 6-8. The amplitude of the annual temperature variation is around 10˚C for all three models. A flux enhancement just near the magnetic equator for L > 1.5 provides a better agreement for all three models.

4. Discussion

The results of the relative fluence estimated from the AP8MAX, AP9 mean and CRRESPRO quiet models are almost identical, as shown in Figure 5, which is rather remarkable. This is due to the equatorial orbit of the Arase satellite (Figure 3). Degradation of the solar cells of the polar orbiting Akebono satellite

was sensitive to the L-shell extent of energetic protons [5] [6], since the satellite integrated particle impact is roughly along the field lines. Therefore, the spatial extent for L-shell among the different models made a clear difference in estimating the degradation of the Akebono solar cells. On the other hand, the orbit of the Arase satellite crosses the field lines especially at low L-shell region where the proton radiation belts exist. This results in sensitivity for particle distribution along the field lines, which is clearly shown in the decreasing RMSE in **Figures 6-8**.

We assumed a steady state for the radiation environment in our study. However, there are reports on the temporal variation of proton radiation by the injection of solar energetic particles and magnetic storms cause the variation [15] [16]. The central part of the proton radiation belt ($L < 2.0$) is rather stable for most disturbances although two exceptional occasions are reported for extreme events [11] [17]. Our interval of analysis between December 2016 and March 2018 was fairly quiet with no large geomagnetic disturbances. The large events were in May and September 2017, where the Dst index reached only −125 and −142 nT, respectively.

Although we only had a few small geomagnetic disturbances, we did encounter an extreme SEP event in the interval of our analysis. The GOES satellite at GEO measured >10 MeV proton flux of 1208/cm^2 s/ster on September 11, 2017. The signature of a large flux of energetic protons can be seen as contamination in the particle detectors on board the Arase satellite. However, we did not see any abrupt change in the estimated Voc (**Figure 2**) or evaluated fluence (**Figure 4**) on that occasion (DOY = 251). Although quite a large flux of energetic protons certainly reached the Arase orbit, the injected energetic protons were not effectively trapped in the inner radiation belt for this event and the fluence was hardly affected. The associated magnetic disturbance seems to have been too small to trap the injected particles. Therefore, a steady state of the proton radiation belt can be a good approximation during the interval of our analysis.

We have so far assumed that trapped protons caused the degradation of solar cells of the Arase satellite. As discussed earlier, we found no evident effects attributable to solar protons. Trapped energetic electrons are another possible cause of the degradation of satellite solar cells. We made model calculations on the energetic electron fluence using the AE8 and AE9 models. We found that due to the outer belt, the variation in increasing relative fluence has an antiphase to that of the trapped protons during the analysis interval. Energetic electrons do not appear to be responsible for the alternating fast and slow periods of increasing relative fluence.

Trapped electrons in the outer belt are highly variable and the Arase satellite has detectors for energetic electrons. We took a quick look at the electron data of the HEP instrument [18] on board the Arase satellite. We found that the electron flux was high around April and October-November in 2017. The relative fluence from the SAP data in **Figures 5-8** (blue lines) shows that the increase was rather small in April (around DOY 100), which is consistent with the model

calculations (red lines) where only trapped protons are considered. In the September-October period (DOY 244-304), the model calculation for protons only (red line) gives an even faster increase in relative fluence compared to that deduced from the SAP data, so an additional contribution of large electron flux would make the deviation larger. Therefore, we conclude that energetic electrons do not significantly affect the particle fluence affecting the degradation of solar cells of the Arase satellite.

We conducted the analysis based on the spatial distribution of trapped protons with energies greater than 6.8 MeV for the CRRESPRO quiet model, and greater than 6.0 MeV for the AP8MAX and AP9 mean models. The range of flight for the cover glass only tells us that energetic protons with energies greater than 6 MeV can damage the solar cells. It is expected that effective damage by energetic protons peaks at around 8 MeV and decreases exponentially with energy. We also made a comparison with models of >8 MeV protons, and obtained almost identical results of the relative fluence for >6 MeV protons.

In this paper, we presented only the results for the case of equatorial proton flux 2.0 times that of the original models for L > 1.5. We have actually tried various modifications with larger/smaller enhancements and different approaches to flux variation along the field line. We found that any flux enhancement on the magnetic equator has the effect of improving the RMSE from that of the original models although the RMSE value varies from one model to another. A long-term variation of proton radiation belt was reported based on data from the Van Allen Probes [19]. Trapped proton flux of 19 MeV and 30 MeV with a pitch angle near 90˚ gradually increased around L = 1.6 to 2.0 from October 2013 to April 2017. Though the data were available only for energies larger than 17 MeV, trapped protons in this region are mainly of SEP origin and similar increase can be probable for >6 MeV protons. We tried steady temporal increase of proton flux just near the equator in our model, and found that any enhancement near the magnetic equator improves the RMSE from the original model. We are not looking further for the best-fitting model based on the minimum RMSE, but simply point out the effect of equatorial enhancement since the deviations appear to have sufficiently vanished from the middle panel (B) of **Figures 6-8**.

The deviation around DOY 50 between the relative fluence deduced from the SAP data and that from the model calculations persists for various models. One possibility to consider is that the satellite was still in the initial operation phase before March 2017. We should have removed data during sequences of special operation, but did not do so in this study. We leave the problem to future analysis. After the satellite shifted to regular operation, coincidence is evident in the middle panel (B) of **Figures 6-8**.

The observation of pitch-angle distribution from the Van Allen Probes suggested that high-energy protons around 26.0 MeV concentrate near the magnetic equator [2]. Particle measurement of the Van Allen Probes has a gap of proton energies between 1 and 17 MeV [3] and thus we cannot make a direct comparison with our results of >6.0 MeV protons. However, observation results of the

Van Allen Probes were obtained at 26.0, 46.0, and 66.0 MeV, and a greater concentration near the equator was found for lower energies. Radiation belt protons of SEP origin are expected to have lower energies and a greater concentration on the equator compared to those of cosmic ray albedo neutron decay (CRAND) origin. Therefore, protons with energies greater than 6.0 MeV are likely to concentrate near the magnetic equator. If we define 30% of the peak flux (broken line) as the outer limit of the equatorial concentration, the extent shown in the bottom panel (C) of **Figures 6-8** roughly corresponds to an equatorial pitch angle larger than about 60˚.

While there is a proton concentration near the magnetic equator, the 10% line of proton distribution extends along the field line off the equator in **Figures 6-8** (C). Trapped protons of CRAND origin are expected to be isotropic and widely spread along the field line. However, it should be noted that our results are significant only around the core portion of proton distribution, *i.e.*, near the flux peak. We analyzed the variation of increasing relative fluence deduced from the degradation of solar cells. The relative fluence mostly results in integration in a large flux region of the proton distribution. Our results are not sensitive to the extent of the low flux region such as low and/or high latitude regions. This point is quite different from the measurement of particle detectors with a wide (usually logarithmic) range of particle flux. Therefore, it would be misleading to draw low flux levels extending toward low and/or high latitude regions by using Equation (1). In this regard, the dotted line (10% of flux peak) in the bottom panel (C) of **Figures 6-8** is probably a fair limit of confidence.

Acknowledgements

We thank all the members of the Arase (ERG) project team for their extensive support.

Conflicts of Interest

The authors declare no conflicts of interest regarding the publication of this paper.

References

[1] Mauk, B.H., Fox, N.J., Kanekal, S.G., Kessel, R.L., Sibeck, D.G. and Ukhorskiy, A. (2013) Science Objectives and Rationale for the Radiation Belt Storm Probes Mission. *Space Science Reviews*, **179**, 3-27. https://doi.org/10.1007/s11214-012-9908-y

[2] Selesnick, R.S., Baker, D.N., Jaynes, A.N., Li, X., Kanekal, S.G., Hudson, M.K. and Kress, B.T. (2014) Observations of the Inner Radiation Belt: CRAND and Trapped Solar Protons. *Journal of Geophysical Research*, **119**, 6541-6552. https://doi.org/10.1002/2014JA020188

[3] Fennel, J.F., Blake, J.B., Claudepierre, S., Mazur, J., Kanekal, S., O'Brien, P., Baker, D., Crain, W., Mabry, D. and Clemmons, J. (2016) Current Energetic Particle Sensors. *Journal of Geophysical Research*: *Space Physics*, **121**, 8840-8858.

[4] Ishikawa, H., Miyake, W. and Matsuoka, A. (2013) Variation of Proton Radiation

Belt Deduced from Solar Cell Degradation of Akebono Satellite. *Earth Planets Space*, **65**, 121-125. https://doi.org/10.5047/eps.2012.06.004

[5] Miyake, W., Miyoshi, Y. and Matsuoka, A. (2014) On the Spatial Extent of the Proton Radiation Belt from Solar Cell Output Variation of the Akebono Satellite. *Advances in Space Research*, **53**, 1603-1609. https://doi.org/10.1016/j.asr.2014.03.002

[6] Miyake, W., Miyoshi, Y. and Matsuoka, A. (2015) An Empirical Modeling of Spatial Distribution of Trapped Protons from Solar Cell Degradation of the Akebono Satellite. *Advances in Space Research*, **56**, 2575-2581. https://doi.org/10.1016/j.asr.2015.10.021

[7] Miyoshi, Y., Shinohara, I., Takashima, T., Asamura, K., Higashio, N., Mitani, T., Kasahara, S., Yokota, S., Kazama, Y., Wang, S.-Y., Tam, S.W., Ho, P.T.P., Kasahara, Y., Kasaba, Y., Yagitani S., Matsuoka A., Kojima H., Katoh, H., Shiokawa, K. and Seki, K. (2018) Geospace Exploration Project ERG. *Earth Planets Space*, **70**, 101. https://doi.org/10.1186/s40623-018-0862-0

[8] Yokota, S., Kasahara, S., Mitani, T., Asamura, K, Hirahara, M., Takashima, T., Yamamoto, K. and Shibano, Y. (2017) Medium-Energy Particle Experiments-Ion Mass Analyzer (MEP-i) Onboard ERG (Arase). *Earth Planets Space*, **69**, 172. https://doi.org/10.1186/s40623-017-0754-8

[9] Knoll, G.F. (1989) Radiation Detection and Measurement. Wiley, New York.

[10] Ginet, G.P., O'Brien, T.P., Huston, S.L., Johnston, W.R., Guild, T.B., Friedel, R., Lindstrom, C.D., Roth, C.J., Whelan, P., Quinn, R.A., Madden, D., Morley, S. and Su, Y.-J. (2013) AE9, AP9 and SPM: New Models for Specifying the Trapped Energetic Particle and Space Plasma Environment. *Space Science Reviews*, **179**, 579-615. https://doi.org/10.1007/s11214-013-9964-y

[11] Gussenhoven, M.S., Mullen, E.G. and Brautigam, D.H. (1996) Improved Understanding of the Earth's Radiation Belts from the CRRES Satellite. *IEEE Transactions on Nuclear Science*, **43**, 353-368. https://doi.org/10.1109/23.490755

[12] Patel, M.R. (2005) Spacecraft Power Systems. Boca Raton, CRC Press.

[13] Kazama, Y. and Goka, G. (2008) A New Modeling Method of Solar Energetic Proton Events for ISO Specification. *Advances in Space Research*, **42**, 1293-1299. https://doi.org/10.1016/j.asr.2007.12.012

[14] Engel, M.A., Kress, B.T., Hudson, M.K. and Selesnick, R.S. (2016) Comparison of Van Allen Probes Radiation Belt Proton Data with Test Particle Simulation for the 17 March 2015 Storm. *Journal of Geophysical Research*: *Space Physics*, **121**, 11,035-11,041. https://doi.org/10.1002/2016JA023333

[15] Lorentzen, K.R., Mazur, J.E., Looper, M.D., Fennel, J.F. and Blake, J.B. (2002) Multisatellite Observations of MeV Ion Injections during Storms. *Journal of Geophysical Research*, **107**, 1231. https://doi.org/10.1029/2001JA000276

[16] Selesnick, R.S., Hudson, M.K. and Kress, B.T. (2010) Injection and Loss of Inner Radiation Belt Protons during Solar Proton Events and Magnetic Storms. *Journal of Geophysical Research*, **115**, Article ID: A08211. https://doi.org/10.1029/2010JA015247

[17] Looper, M.D., Blake, J.B. and Mewaldt, R.A. (2005) Response of the Inner Radiation Belt to the Violent Sun-Earth Connection Events of October-November 2003. *Geophysical Research Letters*, **32**, Article ID: L03S06. https://doi.org/10.1029/2004GL021502

[18] Mitani, T., Takashima, T., Kasahara, S., Miyake, W. and Hirahara, M. (2018) High-Energy Electron Experiment (HEP) Aboard the ERG (Arase) Spacecraft. *Earth Planet Space*, **70**, 77. https://doi.org/10.1186/s40623-018-0853-1

[19] Selesnick, R.S., Baker, D.N., Kanekal, S.G., Hoxie, V.C. and Li, X. (2018) Modeling the Proton Radiation Belt with Van Allen Probes Relativistic Electron-Proton Telescope Data. *Journal of Geophysical Research*, **123**, 685-697. https://doi.org/10.1002/2017JA024661